

Dehydration of Solid $\text{SnCl}_2(\text{OH}_2) \cdot \text{H}_2\text{O}$ to SnCl_2 *

J. Pirnat, J. Lužnik, Z. Jagličić, and Z. Trontelj

IMFM and Physics Department, University of Ljubljana, Slovenia

Z. Naturforsch. **49a**, 367–372 (1994); received August 14, 1993

The temperature and flow rate dependence of the dehydration of $\text{SnCl}_2(\text{OH}_2) \cdot \text{H}_2\text{O}$, having a layered structure, into SnCl_2 in a dry inert gas stream is studied. The experimental results obtained via chlorine NQR and weight measurements are analysed in the light of the structural transformation of this compound. The mechanism of water depletion from the layered structure is discussed.

Key words: Structural transformation, Chlorine NQR, Crystal water, Dehydration modelling, Layered structures.

1. Introduction

Crystalline stannous chloride dihydrate (SCD), more descriptively named dichloroaquatin(II) monohydrate $\text{SnCl}_2(\text{OH}_2) \cdot \text{H}_2\text{O}$ [1, 2], is not a very stable compound. The vapour pressure of its crystal water is appreciable already at room temperature. If the compound is stored in a dry atmosphere or under vacuum it quickly loses water and becomes highly reactive at its surface.

One of the usual methods to obtain anhydrous SnCl_2 powder from polycrystalline SCD is chemical reaction with liquid acetic anhydride [3] followed by purification. Simple drying at elevated temperatures is not recommended because then the product is likely to be unpure owing to partial surface oxydation [4].

Here we present a study of the dehydration of SCD in a stream of a pure inert gas at room temperature and below. There are several possibilities to observe this reaction. The simplest is measurement of the weight loss. Alternative methods are measurement of the disappearing proton NMR signal or measurement of the appearing chlorine NQR signals. The latter method was used here. $\text{SnCl}_2(\text{OH}_2) \cdot \text{H}_2\text{O}$ gives no NQR signal. SnCl_2 samples obtained by the acetic anhydride method [3] exhibit the same chlorine NQR lines as samples dried in an inert gas stream, though the former lines are sharper.

The monoclinic structure of $\text{SnCl}_2(\text{OH}_2) \cdot \text{H}_2\text{O}$ (symmetry $\text{P2}_1/\text{c}$, $Z=4$) [2] is shown in Figure 1 a. Double layers of $\text{SnCl}_2(\text{OH}_2)$ groups are separated by hydrogen bonded layers of crystal water, all the layers being parallel to the bc plane. The structure of anhydrous SnCl_2 , consisting of SnCl_2 chains, is orthorhombic Pnam ($Z=4$), as shown on Fig. 1 b [5]. One kind of chlorine atoms is shared by two equidistant Sn neighbours in a chain. The other kind is coordinated to only one nearest neighbour Sn atom.

Table 1 shows some properties of both compounds.

2. Experimental

Commercial laboratory stannous chloride dihydrate (Fluka) was used. The dehydration was measured at different temperatures between 282 K and 302 K and different flow rates of dry gas between 14 l/h and 105 l/h. The reaction was monitored by weighing of the water loss of the sample and measuring the increasing intensity of the chlorine NQR signal.

The sample compartment for the on-line NQR measurement at low gas flow rate is shown in Figure 2 and that at high flow rate in Figure 3. The dehydration was temporarily interrupted by short intervals (~ 4 min), during which the sample vial was removed, sealed and weighed. Characteristics of the sample are given in Table 2. The NQR measurements were done by pulse spin echo technique. To estimate the resulting amount of SnCl_2 the echo intensity was measured at first. To resolve overlapping lines or to measure the line shape, FFT was applied on the echo signal. Consequently, relaxation and line width measurements were

* Presented at the XIIth International Symposium on Nuclear Quadrupole Resonance, Zürich, July 19–23, 1993.

Reprint requests to J. Pirnat, IMFM, P.O. Box 64 (Jadranska 19), 61111 Ljubljana, Slovenia. Fax: ++38 61 21 72 81; e-mail: z. trontelj@uni-lj.ac.mail.si.



Table 1. Properties of $\text{SnCl}_2(\text{OH}_2) \cdot \text{H}_2\text{O}$ and SnCl_2 .

	$\text{SnCl}_2(\text{OH}_2) \cdot \text{H}_2\text{O}$	SnCl_2
Structure	$\text{P2}_1/\text{c}$	Pnam
Molecular weight	225.6	189.6
Formula-units/cell	4	4
Unit cell volume [nm^3]	0.549	0.318
^{35}Cl NQR lines (287 K) [MHz]*	—	5.84, 4.62
temp. coefficients [kHz/K]*	—	−3.89, −5.95
^{37}Cl NQR lines (287 K) [MHz]*	—	4.60, 3.63
temp. coefficients [kHz/K]*	—	−3.89, −5.95

* scanned interval 282 K to 302 K.

Table 2. Some characteristic data at the beginning of dehydration.

$\text{SnCl}_2(\text{OH})_2 \cdot \text{H}_2\text{O}$ sample mass	3.3 g
$\text{SnCl}_2(\text{OH})_2 \cdot \text{H}_2\text{O}$ sample apparent volume	3.3 cm^3
Bulk crystal specific density	2.71 g/cm^3
Packing ratio of our sample	0.37
Typical grain dimension	0.4 mm
Estimated sample surface area	$240 \text{ cm}^2/\text{g}$

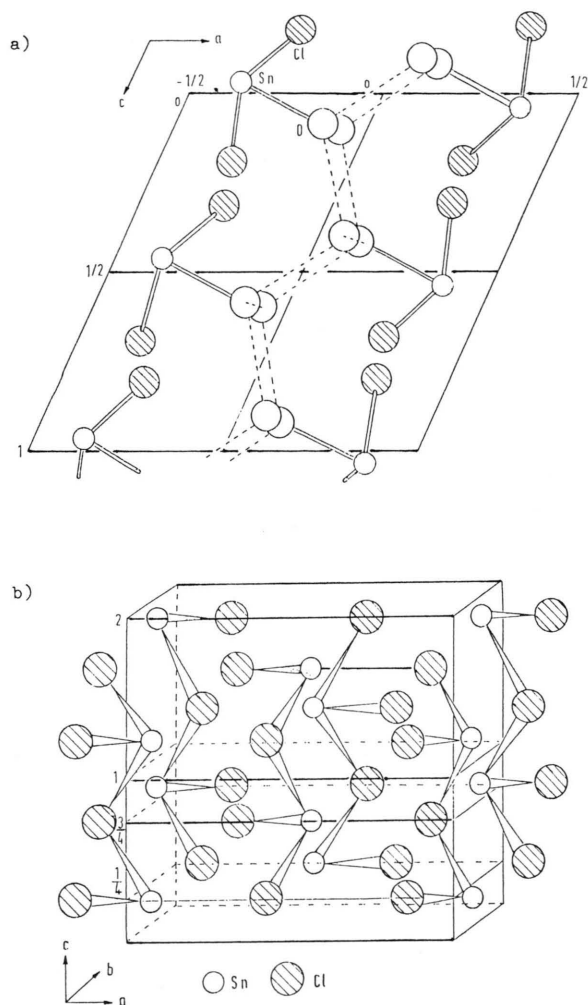
done. Magnetic resonance measurements would have been preferable to weighing because they run simultaneously with the dehydration, but in that case the necessary temperature stabilization of the sample would have been at least 0.1 K or better because the signal intensity is quite temperature dependent.

3. Results and Discussion

If each water molecule of SCD has the same permanent probability to evaporate, their number N decreases with time t according to the equation:

$$\frac{dN}{dt} = -\frac{N}{t_0}, \quad (1)$$

where t_0 is the time constant. In our measurements the weight loss of the sample and/or the chlorine NQR signal intensity has been measured. Both these quantities are denoted by Q in the ratio Q/Q_0 , where Q_0 is the maximum weight loss or maximum NQR signal. Evidently Q/Q_0 equals $1 - \frac{N}{N_0}$, where N_0 is the initial number of water molecules in the SCD sample. t_0 can

Fig. 1. Crystal structures of a) $\text{SnCl}_2(\text{OH}_2) \cdot \text{H}_2\text{O}$ and b) SnCl_2 .

be obtained if the diagram $\log\left(1 - \frac{Q}{Q_0}\right)$ vs. time is linear. The plots are shown on Figure 4. They were recorded at three different flow rates, each set of points representing the time dependence at another temperature. The plots are not linear. In all cases the absolute slope increases with time. To facilitate the comparison of the plots, the fact is exploited that within reasonable limits the evaporation rate is proportional to the gas flow rate. Therefore, a proportional quantity has been chosen for the time scale units, namely the volume of dry gas (N_2) which flew at a constant rate during each experiment. The volume scale and time scale is indicated at the abscissa of the diagrams. The

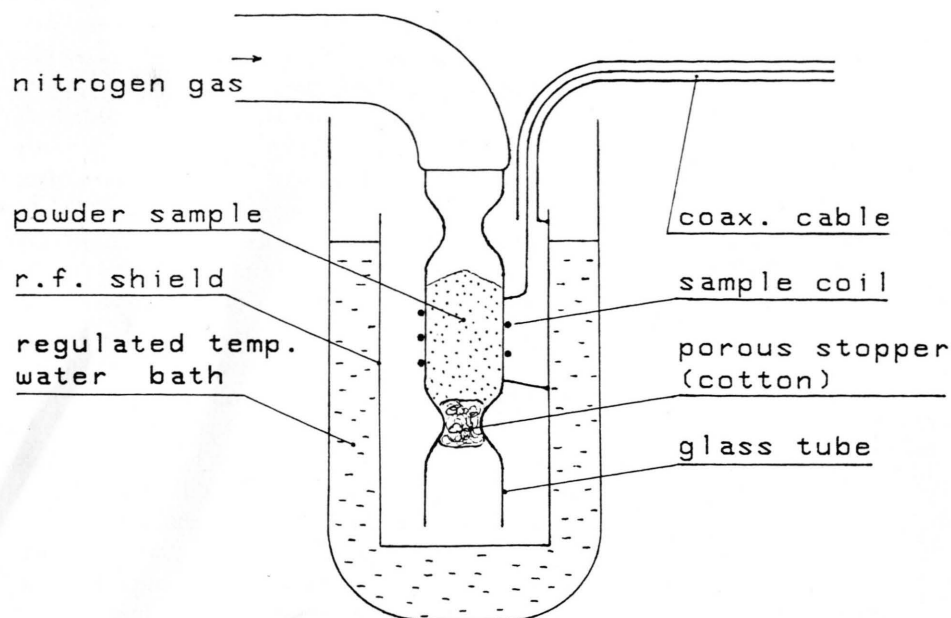


Fig. 2. Sample compartment scheme for simultaneous NQR detection and dehydration.

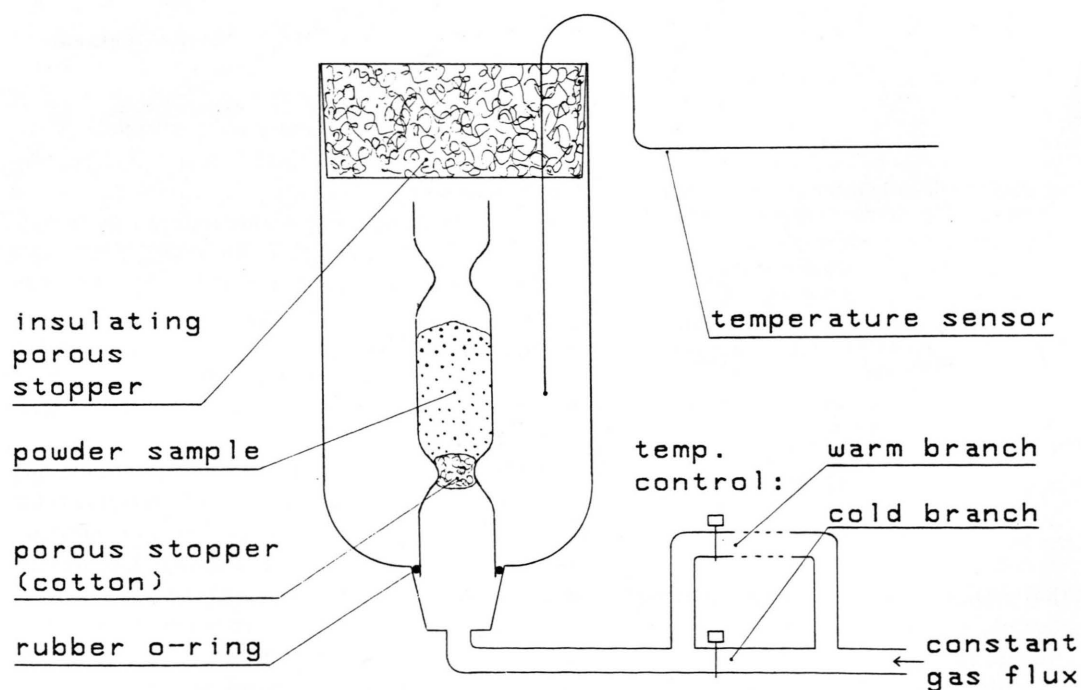


Fig. 3. Experimental set-up for dehydration at higher flow rates.

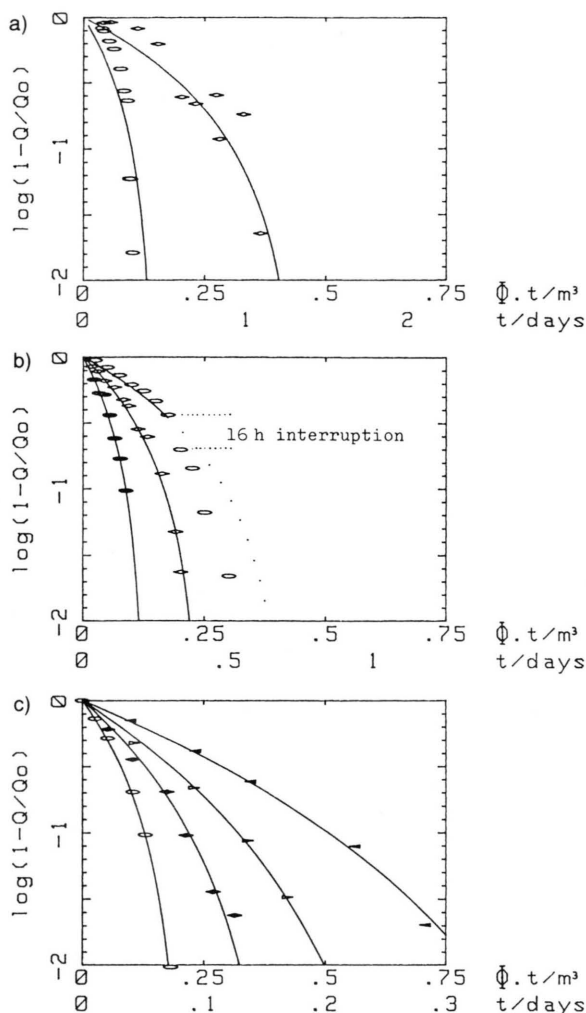


Fig. 4. Semi-log diagrams describing the time (or passed gas volume ϕt) dependence of quantities proportional to SnCl_2 formed.

a) Chlorine NQR signal time dependence at low N_2 flow rate 14 l/h at temperatures 287 K (\diamond) and 302 K (\circ).

b) Time dependence of the mass defect in the sample being dehydrated at medium N_2 flow rate 25 l/h at temperatures 293 K (\circ), 296 K (\diamond) and 299 K (\bullet).

c) Time dependence of the mass defect in the sample being dehydrated at higher N_2 flow rate 105 l/h at temperatures 282 K (\blacktriangle), 287 K (\triangleright), 290 K (\blacklozenge) and 298 K (\circ).

Solid lines represent the time dependence according to (3) (cases a and b) and (5) (case c).

expectation that similar volumes of dry gas are needed for expelling certain percentages of crystal water, no matter what the flow rates are (within our measured interval 14 l/h to 105 l/h), is confirmed in the diagrams on Figure 4.

$\text{SnCl}_2(\text{OH}_2) \cdot \text{H}_2\text{O}$ has a layered structure (see Figure 1a). The mobility of water molecules along the water layers is certainly greater than that normal to the layers. Therefore, evaporation of H_2O molecules is from crystal faces parallel to the bc plane not very probable. SnCl_2 molecules left behind on the surface must recombine into the structure of the anhydrous salt. On the solid SCD surface, probably only very small domains of single crystalline SnCl_2 can be formed, which can qualitatively explain the broad line widths observed for our samples. The newly formed microcrystals of anhydrous salt on the SCD surface are expected to be a negligible obstacle for the next water molecules leaving the SCD surface.

Let us consider a single water layer. The whole crystal behaves as an assembly of similar water layers. The surface from which water molecules can evaporate is proportional to the layer's circumference, which is proportional to the square root of the number of molecules N in the layer. That is more correct than the proportionality to N suggested in (1). The evaporation is then described by

$$\frac{dN}{dt} = -\lambda \cdot N^{1/2} \quad (2)$$

having the solution

$$\frac{N}{N_0} = \left(1 - \frac{t}{t_0}\right)^2, \lambda = 2N_0^{1/2}/t_0. \quad (3)$$

The evaporation proceeds with quadratic decrease of the number of water molecules and it completes in the time t_0 . Notice that t_0 is defined here in a different way than in case of (1).

The diagrams from Fig. 4 were redrawn in the log-log frame (Fig. 5), where (3) is linearized. The points on the diagrams of Figs. 5 a and b₁ approximately follow the straight line according to (3). Scattering of the experimental points in case a is greater, probably due to unstable conditions during the measurement lasting more than 30 hours, and due to the lack of constant sensitivity of NQR measurements. One of the measurements in case b₂ follows the straight line only until the measurement was interrupted for 16 hours, during which the sample was hermetically sealed and kept at room temperature. During this time a redistribution of water molecules seems to have taken place, and after the interruption the dehydration proceeded faster. The consistency of the experimentally determined temperature dependence of the parameter t_0 is acceptable (see Table 3).

Table 3. The product ϕt_0 (ϕ – gas flux, t_0 – time constant from (3)) vs. temperature.

T [K]	302	299	298	295	292	290	287	282
ϕt_0 [m ³]	0.147	0.130	0.208	0.245	0.425	0.416	0.448	1.250

Our attention was attracted by the points on the diagrams of Fig. 5c which also lie on straight lines, but the lower is the temperature the more the corresponding slope deviates from the value 2.

After studying the numerical models of evaporation from two dimensional arrays of particles (to be published) we think of explaining the above mentioned phenomenon by the fractal nature of the boundary of shrinking water layers in an SCD sample being dehydrated.

If we return to (2), assuming that the water layer of N molecules with the global circumference $c \propto N^{1/2}$ possesses a structured boundary (called self-affine surface) with the fractal dimension D [6], then the number of water molecules at the boundary is proportional to $c^D \propto N^{D/2}$, where the fractal dimension of the layer's border is $1 < D < 2$. So, (2) becomes

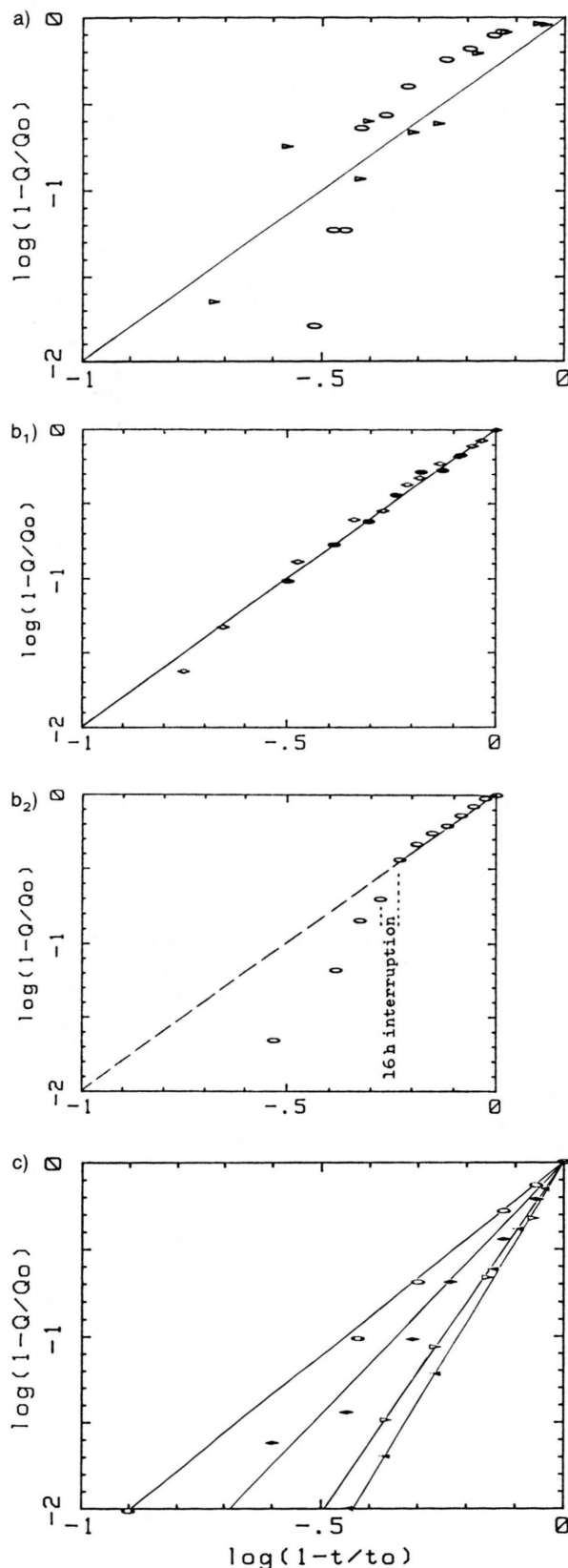
$$\frac{dN}{dt} = -\lambda \cdot N^{D/2} \quad (4)$$

and its solution

$$\frac{N}{N_0} = \left(1 - \frac{t}{t_0}\right)^{2/(2-D)} \quad (5)$$

The slopes of the plots on Fig. 5c give us $D=1.16$ to 1.55 for the corresponding temperatures 298 K to 282 K. That means that D increases with falling temperature. On the other hand, corresponding to lower flow and evaporation rates the value $D=1$ is obtained (Figs. 5a, b). It seems that thermally activated jumps tend to decrease D while accelerated evaporation tends to increase it. In case c the jumps might fail to compete with the evaporation and water layers' boundaries remain rough. With decreasing temperature the jumps of course become still less frequent and the water layer boundaries are more structured, which increases D .

Fig. 5. Log-log diagrams to test the appropriateness of (3) to describe the evaporation: a) case a on Fig. 4, b₁) and b₂) case b on Fig. 4, c) case c on Figure 4. Solid lines represent best fits to (3) and (5), respectively.



- [1] B. Kamenar, D. Grdenić, J. Chem. Soc. **1961**, 3954.
- [2] H. Kiriyaama, K. Kitahama, O. Nakamura, and R. Kiriyaama, Bull. Chem. Soc. Japan **64**, 1389 (1973).
- [3] Organic Synthesis, Vol. **23**, New York 1943, pp. 63–65.
- [4] Gmelins Handbuch der Anorganischer Chemie, Verlag Chemie, Weinheim 1972. No. 46, Part 1, Chapt. 1; p. 193.
- [5] Gmelins Handbuch der Anorganischer Chemie, Verlag Chemie, Weinheim 1972. No. 46, Part 1, Chapt. 1; p. 203.
- [6] T. Visseck, Fractal Growth Phenomena, World Scientific, Singapore 1989, Chapter 7.